

# Performance analysis of a novel rotationally asymmetrical compound parabolic concentrator

Siti Hawa Abu-Bakar [a,b,*], Firdaus Muhammad-Sukki [c,d], Daria Freier [e], Roberto Ramirez-Iniguez [a], Tapas Kumar Mallick [f], Abu Bakar Munir [g,h], Siti Hajar Mohd Yasin [i], Abdullahi Abubakar Mas'ud [j], Norhidayah Md Yunus [k]

[a] School of Engineering & Built Environment, Glasgow Caledonian University, 70 Cowcaddens Road, Glasgow, G4 0BA Scotland, United Kingdom
[b] Universiti Kuala Lumpur British Malaysian Institute, Batu 8, Jalan Sungai Pusu, 53100 Gombak, Selangor, Malaysia
[c] School of Engineering, Faculty of Design and Technology, Robert Gordon University, Garthdee House, Garthdee Road, Aberdeen, AB10 7QB, Scotland, United Kingdom
[d] Faculty of Engineering, Multimedia University, Persiaran Multimedia, 63100 Cyberjaya, Selangor, Malaysia
[e] Faculty 1 Renewable Energies, University of Applied Sciences, Treskowallee 8, 10318 Berlin, Germany
[f] Environment and Sustainability Institute, University of Exeter, Penryn, Cornwall, TR10 9EZ, United Kingdom
[g] Faculty of Law, University of Malaya, 50603 Kuala Lumpur, Malaysia
[h] University of Malaya Malaysian Centre of Regulatory Studies (UMCoRS), University of Malaya, 5990 Jalan Pantai Baru, Kuala Lumpur, Malaysia
[i] Faculty of Law, Universiti Teknologi MARA, 40450 Shah Alam, Malaysia
[j] Department of Electrical and Electronic Engineering Technology, Jubail Industrial College, P O Box 10099, Saudi Arabia
[k] Department of Real Estate, Faculty of Geoinformation and Real Estate, Universiti Teknologi Malaysia, 81310 Skudai, Johor, Malaysia
* Phone/Fax number: +44(0)141 273 1482/+44(0)141 331 3690, e-mail: sitihawa.abubakar@gcu.ac.uk/ hawa012@gmail.com

**Abstract**: The low-concentration photovoltaic (LCPV) system has been identified as one of the potential solutions in lowering the overall installation cost of a building integrated photovoltaic (BIPV) system. This paper evaluates the performance of a novel type of LCPV concentrator known as the rotationally asymmetrical compound parabolic concentrator (RACPC). A specific RACPC design with a geometrical concentration ratio of 3.6675x was fabricated and integrated with a 1 cm by 1 cm monocrystalline laser grooved buried contact silicon solar cell. This design was tested indoors to evaluate its current-voltage (I-V), angular response and thermal characteristics. Under standard test conditions, it was found that the RACPC increases the short circuit current by 3.01x and the maximum power by 3.33x when compared with a bare solar cell. The opto-electronic gain from the experiment showed good agreement when compared with the simulation results, with a deviation of 11%.

**Keywords:** solar photovoltaic; solar concentrator; rotationally asymmetrical compound parabolic concentrator.

## 1. Introduction

Solar photovoltaic (PV), which is one of the technologies that harnesses solar energy by converting the sunlight directly into electricity, grew by more than 100 folds from 2000 to 2013, with a cumulative capacity of 139 GW by the end of 2013 [1]. One of the reasons for this growth has to do with the fact that the governments of several countries have taken the right steps to stimulate the adoption of solar PV technologies. With regards to policy one of the most effective ones is known as the feed-in tariff (FiT) scheme [2–13]. This scheme pays a consumer a specific tariff per kWh of electricity generated from solar PV technology for a duration of time [8], and is now being enacted in more than 80 countries [2].

Despite the growth of solar PV, the Intergovernmental Panel on Climate Change (IPCC) indicates that 'its share of primary energy supply has remained relatively constant' [14]. Therefore more needs to be done to ensure that renewable technologies, especially solar PV, are more widely adopted in order to reduce climate change.

One of the problems that surrounds the PV technology is its high cost of implementation, which according to the recent data from the International Energy Agency (IEA) ranged between £830 and £16,000 per kW [1] [15]. The largest proportion of the cost (approximately 45%) was due to the expensive PV material used in the fabrication of the module [15]. It is argued that by reducing the usage of PV material in a PV module, it is possible to achieve a cheaper PV system, which could further attract more consumers into opting and installing this technology [16–18].

A possible way to reduce the amount of expensive PV material and therefore the cost of the PV modules and the PV systems is by using a solar concentrator – a device (mainly constructed from a low cost refractive and/or reflective material) that focuses the solar radiation from a large entrance aperture area into a smaller exit aperture where a solar cell is attached [16–18]. This allows the system to generate a similar or higher electrical output than a conventional PV system, while at the same time using only a fraction of the PV material.

Several researchers have explored various concentrator designs since the late 1960s. A low-concentration photovoltaic (LCPV)[2] system is more suitable for building integration since it has a wider half-acceptance angle which eliminates the need for any

[1] Based on the conversion rate carried out on 10/11/2014, USD1.00 is equivalent to £0.63 [50]. This value is used throughout this paper.

[2] An LCPV is as a system that incorporates a concentrator with a geometrical gain of less than 10x.

electromechanical tracking of the sun [19,20], it increases the optical gain under both direct and diffuse radiation [19] and it does not require any active cooling requirement [21]. Uematsu *et al.* [22] developed a flat-plate static concentrator (FPSC) that was able to increase the maximum power output by 2% when compared with a conventional PV module. Gajbert *et al.* [23] studied a reflective parabolic concentrator and calculated that the design could boost the annual electricity production by 72% compared to a non-concentrating design. Garcia *et al.* [24], on the other hand, experimented on a V-trough concentrator and obtained a maximum power gain of up to 1.5 when compared with a non-concentrating panel. Yoshioka *et al.* [25] constructed a 3D refractive static concentrator and obtained an optical gain of 2.3x when compared with a bare cell. Muhammad-Sukki *et al.* [18,26–31] investigated the performance of an extrusion of a dielectric totally internally reflecting concentrator (DTIRC) and concluded that their design could increase the electrical output by nearly 5 times when compared with a non-concentrating system. Ramirez-Iniguez *et al.* [32] patented a variation of the DTIRC, which is a rotationally asymmetrical DTIRC and have demonstrated that their design could achieve an opto-electronic gain of 4.2x when compared with a bare PV cell [33–36]. Mallick and Eames [37] investigated a reflective asymmetrical compound parabolic concentrator (CPC) which improved the power concentration ratio of the panel by 2.1 times when compared with a similar non-concentrating panel. Another CPC design studied by Mammo *et al.* [37] known as the crossed compound parabolic concentrator (CCPC) generated 3 times more maximum power than the one generated by a non-concentrating system.

This paper proposes a new variation of CPC design for use in building integrated photovoltaic (BIPV) systems. This concentrator is known as a rotationally asymmetrical compound parabolic concentrator (RACPC). This paper aims at evaluating the electrical performance of the concentrator under standard test conditions. The process to design the concentrator as well as the theoretical and simulation work related to this concentrator design have already been covered in detail by the authors in [38]. Section 2 summarises the steps involved in the design of the concentrator. The fabrication and assembly of the prototype is discussed in section 3. The experimental setup is discussed in Section 4. Section 5 presents a discussion of the results from the experiments, and finally the conclusions are presented at the end of the paper.

## 2. RACPC Design

The RACPC is a new variation of the CPC. The design utilised similar algorithms to generate the dielectric totally internally reflecting concentrator (DTIRC) by Ning et al. [39], in which they proved that the CPC is a DTIRC with a flat entrance aperture. A MATLAB® code was written to create the RACPC by taking into account the desired input parameters: the total height of the concentrator, (*HTot*), the half-acceptance angle ($\theta_a$), the length of the PV cell ($L_{PV}$), the width of the PV cell ($W_{PV}$), the trial width of the entrance aperture ($d_1$), the index of refraction of the material ($n$) and the number of extreme rays ($N$).

The steps in producing this design has been presented in detail in [38]. Figure 1 helps to explain the process to design the RACPC. Based on the input parameters, the MATLAB® programme produces the first 2D-symmetrical design, which is plotted at 'Position 1' in Figure 1. Then , a new CPC design is produced, with each new design is computed by incrementing the angle of rotation of the cross-sections by 1º and by using the predetermined exit aperture value (see 'Positions 2, 3 and 4' in Figure 1). The process stops when a 180° rotation around the y-axis is completed. The programme generates the point cloud coordinates of the RACPC and obtains some important parameters of the design, i.e. the geometrical concentration gain, the half-acceptance angle and the maximum width of the entrance aperture of the concentrator.

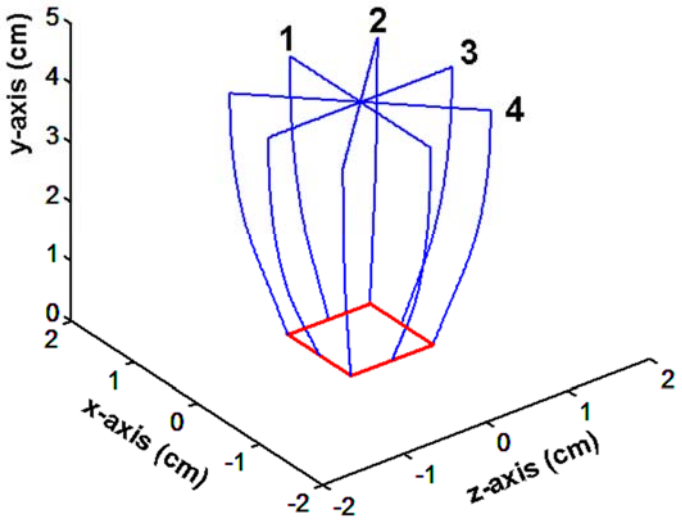


Figure 1: Demonstration of the angular rotation of the 2-D cross-sections to produce the RACPC.

## 3. Prototype Fabrication and assembly

As explained above, a MATLAB® code was written to generate the point cloud coordinates of the RACPC and these Cartesian coordinates were then transferred into the GeoMagic® software to produce a Computer-Aided Design (CAD) file. The CAD file was sent to UK Optical Plastics Limited, United Kingdom [40] for the fabrication of a prototype using a single-point diamond turning process. Photographs of the prototype of the concentrator are presented in Figure 2. This design has a geometrical concentration ratio of 3.6675, a total height of 3cm, an exit aperture of 1cm by 1cm and an entrance aperture width of 2.0598cm along both the x and z-axis.

The material for the fabrication of the prototype was Altuglas® V825T, a variation of the polymethyl methacrylate acrylic (PMMA) resin, which has a refractive index of 1.49 [41]. PMMA is a widely used material for optical concentrators due to its high transmittance (92%) and good resistance to photo degradation [42].

The RACPC has unique features and advantages when compared with conventional CPC designs. These include [38]:

1. It has a flat entrance aperture with four axis of symmetry (see Figure 2(b)), unlike the 3-D rotationally symmetry CPC or the CCPC which has a circular and square/rectangular shape respectively. By having a flat entrance aperture, an array of these concentrators can be moulded with a thin layer of material (the same material that produces the concentrators) joining them together. This will ease the assembly process [20,43] and potentially reduce the assembly cost of the system.
2. It has a square exit aperture, as presented in Figure 2(d), which could easily match a square solar cell. A square or rectangular cell is easier to manufacture [37] and therefore it is the most commonly available shape in the market, unlike a circular cell needed by a rotationally symmetry CPC design.
3. It is also considered as a 3D design, hence it provides concentration on both planes perpendicular to the propagation of light along the concentrator axis and a higher geometrical concentration gain than the 2D linear CPC design.

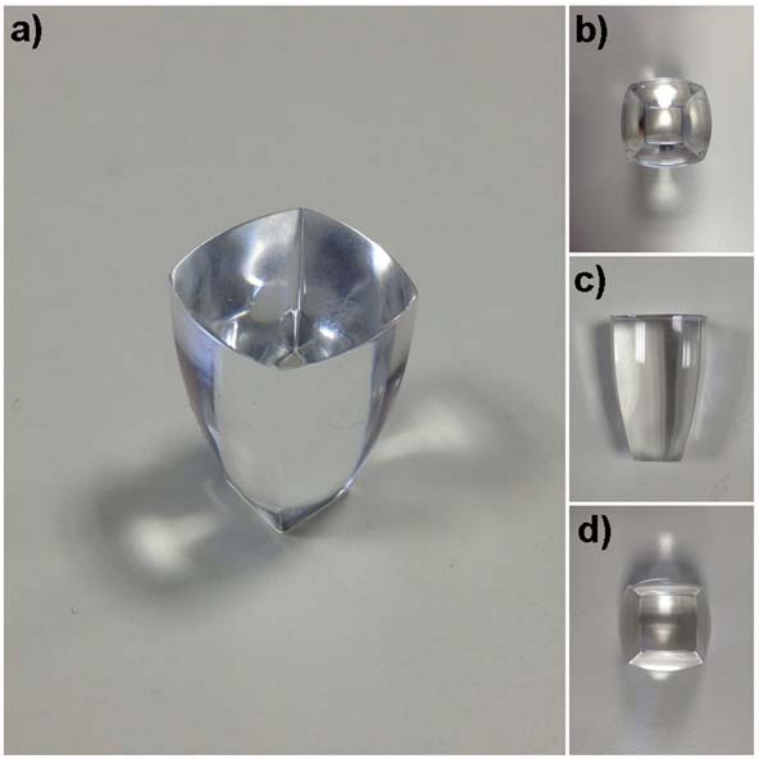


Figure 2: The RACPC prototype fabricated for experimental purposes, where (a) is the isometric view; (b) is the top view; (c) is the side view, and (d) the bottom view of the concentrator.

Two solar cells were used for the test of the RACPC. These were supplied by Solar Capture Technologies Ltd, United Kingdom [44] and each one has an active area of 1 x 1 cm. These monocrystalline Laser Grooved Buried Contact (LGBC) silicon solar cells are suitable for LCPV applications [44]. The cells were tabbed with a lead free wire of 0.1mm thickness and 1mm width using a soldering iron of 81W and a heat temperature of 350°C. To ensure that the active area for each cell is 1 x 1 cm, the tabbing wire was placed as close to the edge as possible. The cells were then glued on two separates glass substrates (70mm x 70mm x 4mm) and one of them was assembled permanently with the RACPC.

To mount the RACPC on the solar cell, a silicon elastomer Sylgard-184® from Dow Corning was chosen as the binding material. This material also acts as an encapsulation material for the solar cell and as an index matching gel between the concentrator and the cell [34]. It has a high transmittance value (90%) and can be cured using a simple process [20,34,42]. The Sylgard-184® was prepared by mixing the supplied base and curing agent in a 10:1 weight ratio in a small beaker. The mixture was then placed in a vacuum chamber for 15 minutes to eliminate air bubbles. A Dow Corning Primer 92-023 was then applied on the solar cell for a better adhesion between the Sylgard and the cell. Once the Sylgard was free

from air bubbles, the mixture was poured on top of the tabbed cell. Afterwards, the RACPC was placed carefully on top of the solar cell and the elastomer was left to cure for 48 hours under room temperature to ensure good binding between the RACPC and the cell. Figure 3 shows the prototype of the RACPC-PV structure.

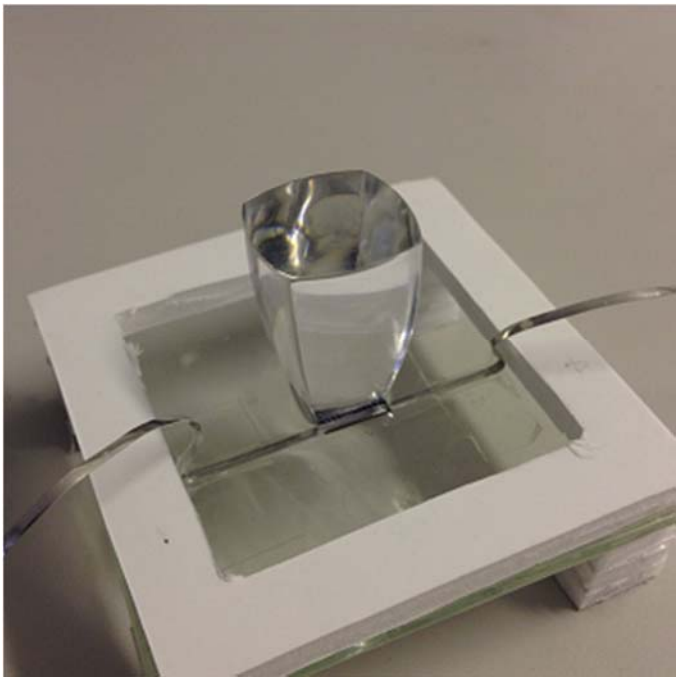

Figure 3: The prototype of RACPC-PV structure.

## 4. Experimental setup

The indoor experimental setup to evaluate the characteristic of the RACPC is illustrated in Figure 4. A Class AAA solar simulator (Oriel® Sol3A Model 94083A) from Newport Corporation equipped with an AM 1.5G filter, was used to reproduce the spectral emission of the sun at the earth surface, providing a uniform illumination with a marginal error of ±2%. A variable slope base was placed approximately 38cm beneath the solar simulator's lamp and within the uniform illumination area (20cm x 20cm) of the lamp. The variable slope base was used together with a digital tilt meter to accurately measure the tilt angle of the base. A Keithley source meter (Model 2440) with 4-wire connections was utilised here to act as a high accuracy loading circuit [34,36]. The source meter was connected to a computer which has already been installed with the Lab Tracer software from

National Instruments® to measure the electrical output from the PV cells. The RACPC was placed on the variable slope base set at 0º inclination. Under standard test conditions (STC), the solar simulator was configured to produce an irradiance of 1,000 W/m$^2$ and the room temperature was maintained at 25°C. The door and windows of the room were closed to avoid unwanted air flow and minimise temperature variations and the room windows had blinds to prevent unwanted light from entering the room. In order to obtain the current-voltage and power voltage curves of the concentrated-PV cell (and of the bare cell), and from these characterise the angular variation of the optoelectronic gain of the concentrator, the sample (RACPC-PV or the non-concentrating cell) was exposed to the solar simulator light for short periods of time (approximately 5s) using a shutter. This was done to minimise the increase in the solar cell's temperature which would have affected the readings of the open circuit voltage and the fill factor. For each measurement, the short circuit current ($I_{sc}$), the open circuit voltage ($V_{oc}$), the maximum current ($I_{max}$), the maximum voltage ($V_{max}$), the maximum power ($P_{max}$) and the fill factor ($FF$) were determined and recorded. The performance of the RACPC and the non-concentrating cell were evaluated for these cases: (i) under STC at 0º inclination; (ii) under STC at different angle of incidences between -60º and 60º, (iii) under various solar radiations at 0º inclination, and (v) under long exposure to constant radiation of 1000W/m$^2$ at 0º inclination.

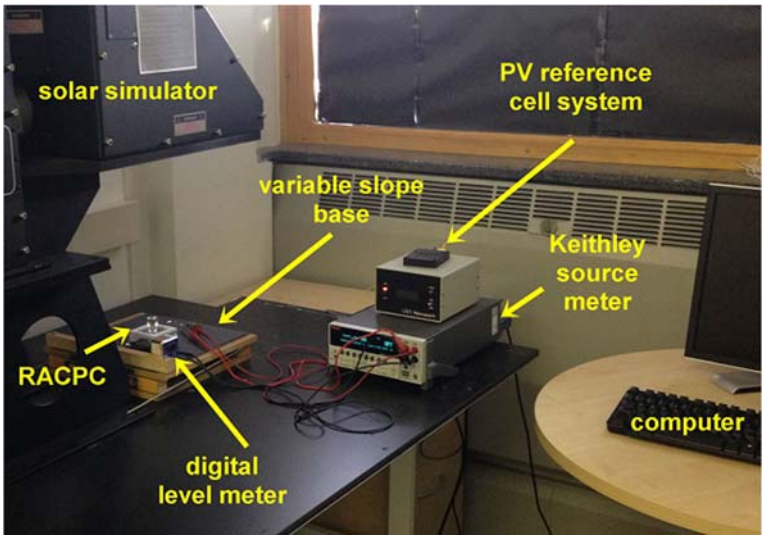


Figure 4: Indoor experimental setup.

## 5. Results and discussions

### 5.1 The characteristic of the RACPC under STC at 0º inclination

Figure 5 shows the current-voltage (I-V) characteristic and the power-voltage (P-V) characteristic of the RACPC under STC. From Figure 5, the short circuit current of the bare cell was recorded at 35.5mA. However, the introduction of the RACPC in the design increased the short circuit current by a factor of 3.01 when compared with the bare cell, generating 107.0mA. As indicated earlier, the concentrator was concentrating the irradiance from the entrance aperture to the exit aperture. This increased the intensity of the light that impinged on the solar cell linearly [45], resulting in a higher short circuit current than the one produced from the bare cell. The open circuit voltage was also increased from 0.560V to 0.565V when the RACPC was compared with a non-concentrating cell. Unlike the short circuit current, the open circuit voltage increased logarithmically with irradiance concentration [45]. The maximum power on the other hand was increased from 0.015W to 0.050W when the RACPC was compared with the bare cell, giving a maximum power ratio of 3.33. The experiment showed that the RACPC increased the fill factor from 77% to 79%. The fill factor increased due to an increase in both the short circuit current and the open circuit voltage of the concentrator.

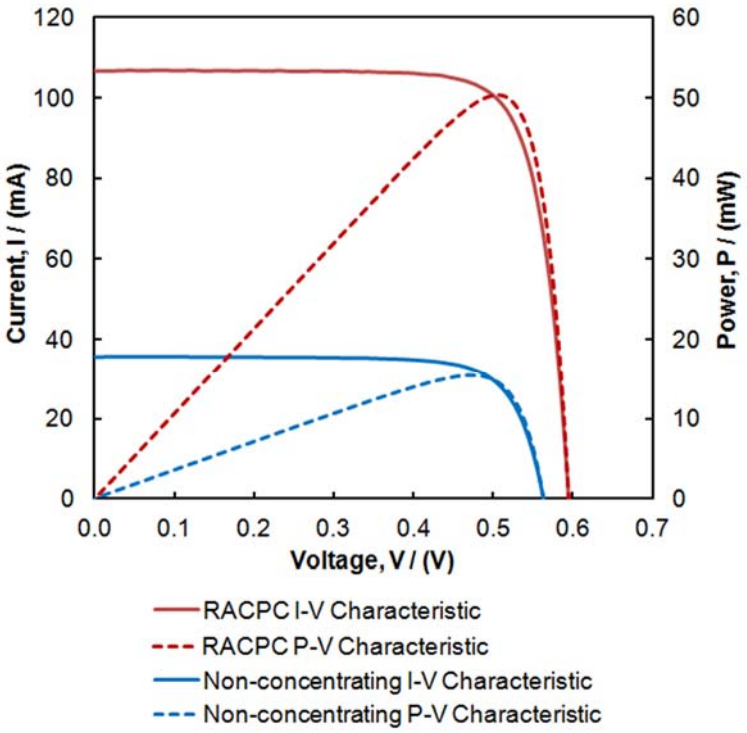


Figure 5: (I-V) and (P-V) characteristics of the RACPC and the bare cell under standard test conditions.

240 5.2 The angular response of the RACPC under STC

241

242 The next part of the experiment consisted in characterising the angular response of the
243 RACPC. This experiment evaluates the electrical performance of the system when the sun
244 path varies throughout the day. Instead of tilting the source, the variable slope base was tilted
245 from 0° to 60° at increments of 5°, with each tilt angle measured using the digital level meter.

246 Figure 6 compares the short circuit current generated by the RACPC with the ones
247 generated by the bare cell for angles of incidence within the ±60º range. In general, the short
248 circuit current showed a decreasing trend when the angle of incidence increased. In Figure 6,
249 at normal incidence, the RACPC generated the maximum value of short circuit current,
250 107.0mA, which was 3.01x higher than the 35.5mA short circuit current generated by the
251 non-concentrating cell. The short circuit current from the RACPC reduced to 50% of its peak
252 value when the angle of incidence was ±43º, and continued to drop when the angle of
253 incidence increased. However, it was observed that the short circuit current generated from
254 the RACPC was always higher than the one generated from the bare cell when the angle of
255 incidence was within ±50º. As for the bare cell, although the short circuit current value
256 reduced when the angle of incidence increased, it showed a gradual dropped from its peak
257 value. It achieved 50% of its maximum short circuit current value when the angle of
258 incidence was approximately ±60º. This reduction was contributed mainly due to the cosine
259 effect[3] [20,46].

260

[3] The cosine angle effect occurs when the surface of a flat solar cell is not normal to the sun radiation (in this case the solar simulator's radiation), the effective value of the sun radiation exposed to the cell will be reduced by the cosine of the angle between the sun and the cell's normal [46].

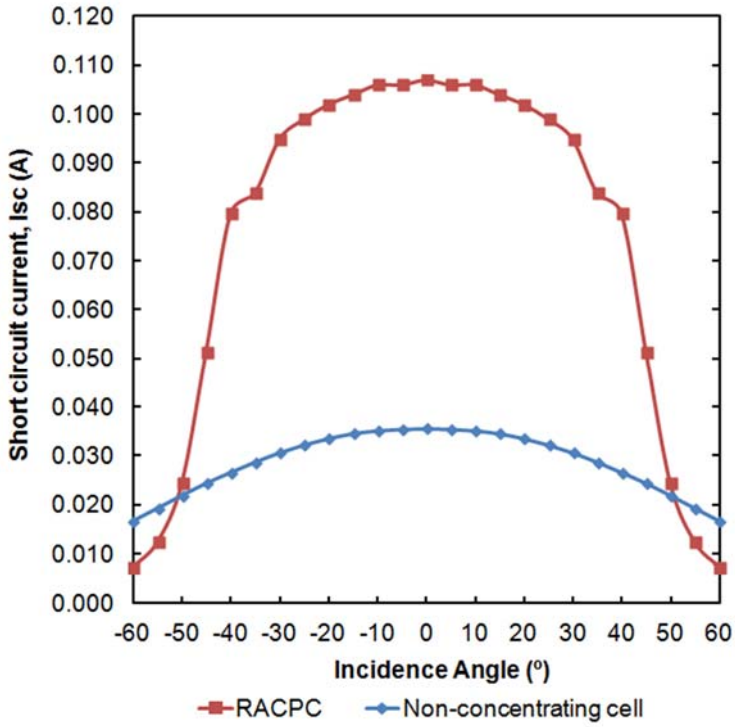


Figure 6: The short circuit current variation of the RACPC and the bare cell at different angles of incidence.

There are two ways to investigate the performance of the concentrator. One is by looking at the opto-electronic gain of the concentrator, and the other is by analysing its optical efficiency. The opto-electronic gain measures the ratio of short circuit current produced from an LCPV device to the one generated from a non-concentrating cell [20,34,39]. The optical efficiency, on the other hand, is obtained by dividing the opto-electronic gain by the RACPC's geometrical concentration ratio value [37,47]. A higher opto-electronic gain is desirable since it translates into a higher short circuit current, while a higher optical efficiency means that a higher percentage of the rays that fall on the front surface area are transmitted to the exit aperture of the concentrator. From the opto-electronic gain, the half-acceptance angle of the RACPC was determined, which is defined as the angle where the gain reached 90% of its peak value [37]. The opto-electronic gain and the optical efficiency of the RACPC are presented in Figures 7 and 8 respectively.

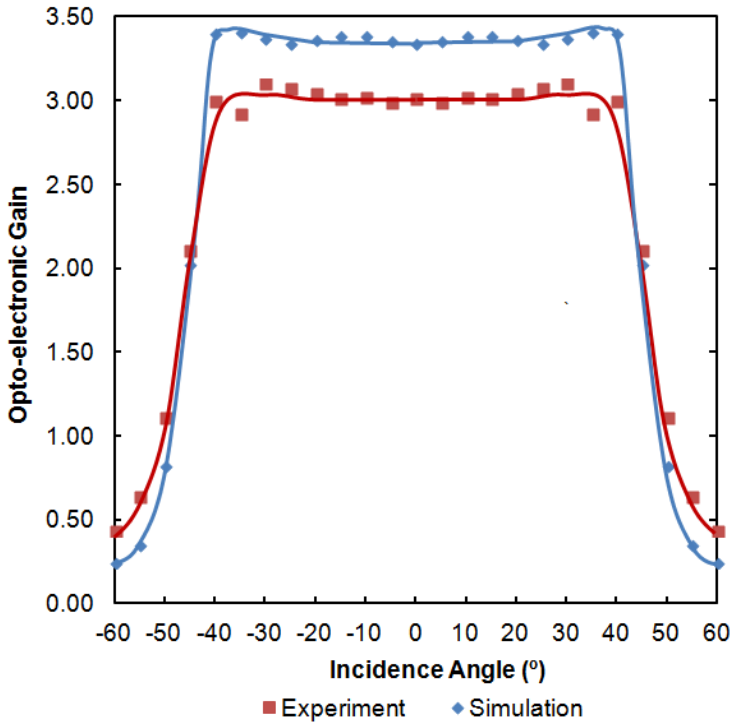


Figure 7: The opto-electronic gain of the RACPC at different angles of incidence.

As it can be observed in Figure 7, the opto-electronic gain value remains fairly constant at approximately 3 when the angle of incidence increased from 0 to ±40º, and dropped to 90% of its peak value when the angle of incidence reached ±43º. Beyond this angle, the opto-electronic gain suffered a sudden drop to almost 0. According to Sarmah *et al.* [20], the short circuit current of a concentrator drops when the angle of incidence is getting closer to (and higher than) the value of half-acceptance angle of the concentrator because of rays escaping from the side profile of the concentrator as well as at the concentrator-encapsulation interface. It was also observed that some the instantaneous opto-electronic gain readings within the acceptance angle were higher than the ones recorded at normal incidence. This was contributed to the rays impinging the side profile of the concentrator arrived at the solar cell. The opto-electronic gain variation was compared with the optical gain obtained from the simulations. The simulations were carried out using an optical analysis software ZEMAX® and the detail simulation steps have been presented in [38]. The opto-electronic and the optical gain were plotted together in Figure 7. A similar trend was observed in the ray-tracing simulation. Here, the half-acceptance angle was recorded to be ±42º, which shows good agreement between the experimental and the simulation results. Interestingly, the half-

acceptance angles of the RACPC determined from the experiment and the simulation were also very close to value calculated from the MATLAB® program, which was ±42.9578º. Table 1 shows the comparison of the most important parameters obtained from the MATLAB® programme, the experimental work and the ray-tracing simulations.

Table 1: Comparison of parameters obtained from MATLAB®, ZEMAX simulation and experiment.

| | MATLAB | Simulation | Experiment |
|---|---|---|---|
| Geometrical gain | 3.6675 | - | - |
| Optical/Optoelectronic gain (at 0°) | - | 3.4 | 3.0 |
| Optical efficiency (at 0°) | - | 92% | 84% |
| Acceptance angle (°) | ±42.9578 | ±42 | ±43 |

The variation of the optical efficiency of the RACPC with angle of incidence is presented in Figure 8. From the experiments, the RACPC achieved an 84% optical efficiency at normal incidence, and this value dropped to 90% of its maximum value when the angle of incidence of the rays was ±43º. Outside this range of incidence angle, the optical efficiency dropped to 0%. The optical efficiency trend from the experiments was compared with the simulations carried out in ZEMAX® [38]. The experiments show good agreement with the ray-tracing simulations, with a deviation of 11%. The deviation occurred due to several factors including (i) manufacturing errors causing the dimensions of the concentrator to differ from the actual design dimensions, uneven surfaces of the entrance aperture and over polishing on the profile of the side wall; (ii) assembly errors during the soldering of the tabbing wire on the solar cells, which reduced the effective area of each cell, and misalignment between the solar cell and the exit aperture of the concentrator, and (iii) errors associated with the rays such as scattering, absorption of the material and reflection on the front surface of the concentrator which reduces the number of rays reaching the exit aperture of the RACPC.

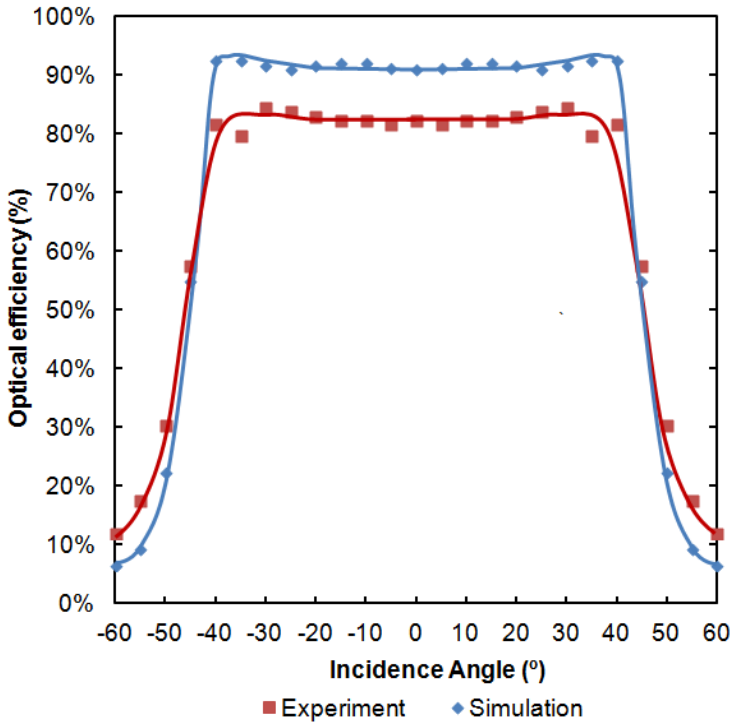


Figure 8: The optical efficiency of the RACPC at different angles of incidence.

In terms of the variation of the maximum power output with angle of incidence, a similar trend to the one obtained for the short circuit current was observed, as illustrated in Figure 9. The peak value of the maximum power was recorded at 0.050W and 0.015W from the RACPC and the non-concentrating cell respectively. This translated to a maximum power ratio (power gain) of 3.33. The maximum power generation of the RACPC reached 50% of its peak value when the angle of incidence was ±44º, before gradually dropping to 0W when the angle of incidence continued to increase. As for the maximum power from the bare cell, the reduction of the maximum power was more gradual, achieving a 50% of the peak value when the angle of incidence was closer to ±60º.

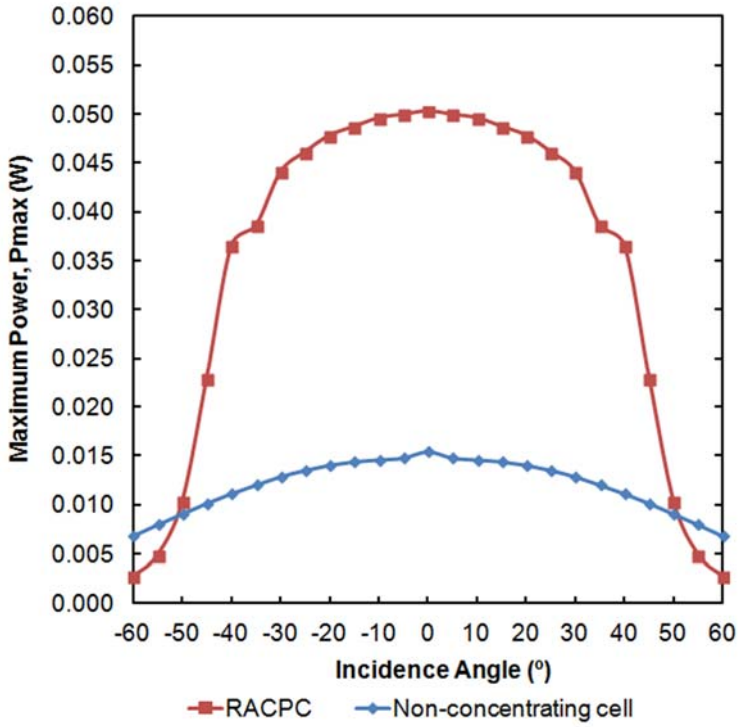


Figure 9: The maximum power variation of the RACPC and the bare cell at different angles of incidence.

5.3 Variation of solar irradiance at 0º inclination at 25°C.

The experiment was repeated to evaluate the variation of the I-V and P-V characteristics under various level of solar radiation. This investigation is helpful to evaluate the performance of the RACPC in locations that have higher or lower average levels of solar irradiance. This was done by turning the variable attenuator control of the solar simulator to change its output from 800 W/m$^2$ to 1100W/m$^2$, at increments of 100W/m$^2$. The results are presented in Figures 10 and 11. When the intensity of the solar simulator increased from 800 W/m$^2$ to 1100W/m$^2$, the short circuit current from both samples increased from 0.085A to 0.117A for the RACPC and from 0.028A to 0.039A for the bare cell. In terms of maximum power, the change in the simulator's intensities caused the reading from the samples to rise from 0.040W to 0.056W and from 0.012W to 0.017W for the RACPC and the bare cell respectively. In general, the RACPC produces a higher short circuit current and a higher maximum power when exposed to higher level of solar radiation, as expected, which is more desirable by the consumers that want to reap higher financial return from the FiT scheme.

However, a long exposure to high irradiance increases the cell's temperature, and reduces the maximum power generated from the cell [34]. The next section evaluates the effect of temperature on the cell's performance when exposed to the same irradiance over a long period of time.

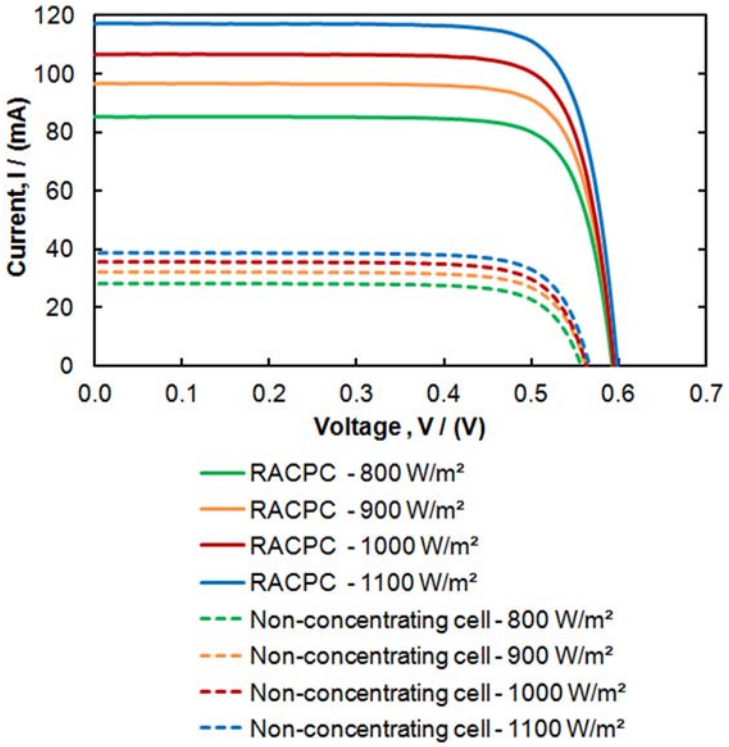


Figure 10: The I-V characteristic of the RACPC and the bare cell under various levels of irradiance.

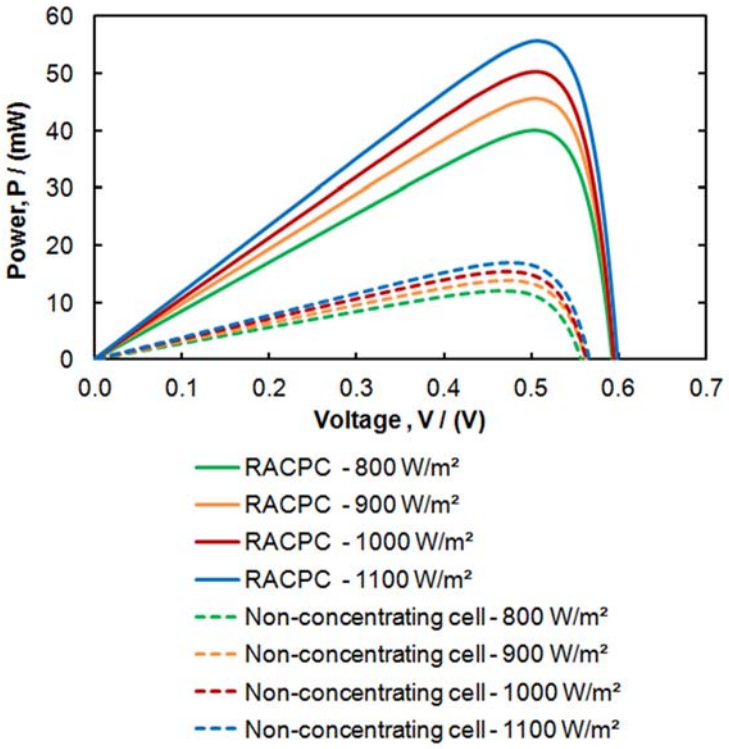


Figure 11: The P-V characteristic of the RACPC and the bare cell under various levels of irradiance.

## 5.4 The thermal characteristic of the RACPC

This section evaluates the effect of temperature on the performance of the RACPC panel. Two thermocouples were utilised; one was attached to the back of the glass substrate exactly beneath the solar cell to measure the cell temperature, and another one exposed to the air to measure the room temperature. Each thermocouple was connected to an ammeter. Next, the RACPC was placed at 0° of inclination. The solar simulator was then configured to produce 1000 W/m$^2$ and the room temperature was set at 25°C. The RACPC was exposed to the same radiation for a period of 4.5 hour and a set of reading was taken every 15 minutes.

Figure 12 shows the effect of temperature on the maximum power of the RACPC. The temperature of the cell increased sharply from 25°C to 57°C and stabilised after 2.75 hours. The maximum power was reduced from 51mW to 44mW, a reduction of 13.7%. Table 2 presented the variations of parameters throughout the duration of the experiment. The maximum voltage showed a large fall from 0.51V to 0.44V. The increase in temperature caused the semiconductor band gap to decrease [48]. This enabled more incident energy to be absorbed by the semiconductor which translated to a lower energy needed to move the

carriers into the conduction band [48]. As a result, this phenomenon produced more photocurrent through the semiconductor which consequently reduced the open circuit voltage [48]. No change was recorded to the maximum current value. As for the fill factor, the value dropped from 80% to 77% which occurred due to the drop in open circuit voltage reading.

It is therefore crucial for an LCPV system to have the right RACPC design and cooling system to ensure that the performance of the solar cell is at its optimum. If an RACPC design with higher gain is needed, the solar cell could be cooled by introducing a hybrid/thermal system (either using air or water), that utilises the co-generated heat to produce hot water and stimulate ventilation [26,33,49].

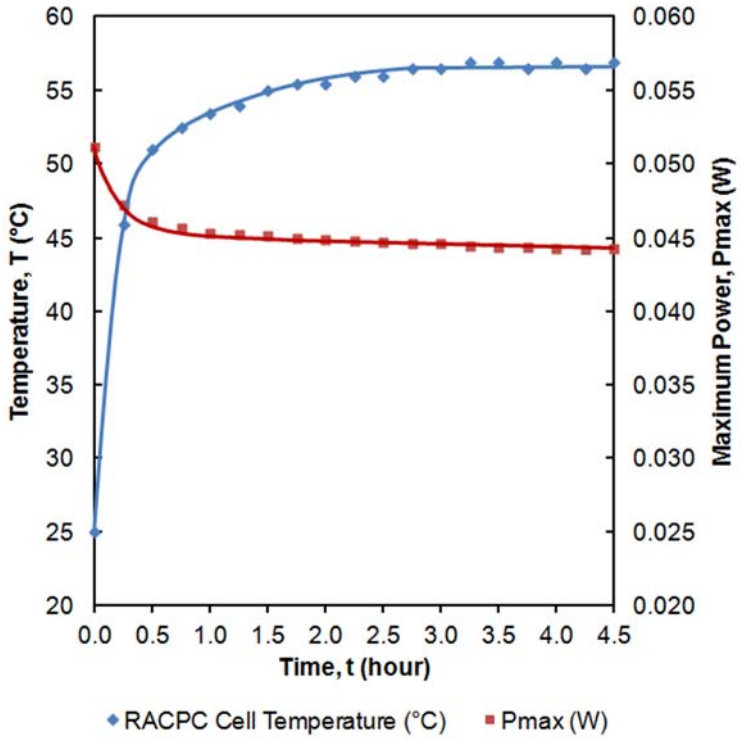


Figure 12: The variation of the maximum power and the RACPC cell temperature with illumination time.

Table 2: Effect of temperature on the RACPC output.

| Time (hour) | Room Temperature (°C) | CPV Temperature (°C) | Vmax (V) | Imax (A) | Pmax (W) | Voc (V) | Isc (A) | FF |
|---|---|---|---|---|---|---|---|---|
| 0.00 | 25 | 25 | 0.51 | 0.10 | 0.051 | 0.60 | 0.11 | 0.80 |
| 0.25 | 25 | 46 | 0.47 | 0.10 | 0.047 | 0.56 | 0.11 | 0.78 |
| 0.50 | 26 | 51 | 0.46 | 0.10 | 0.046 | 0.55 | 0.11 | 0.77 |
| 0.75 | 26 | 53 | 0.46 | 0.10 | 0.046 | 0.55 | 0.11 | 0.77 |
| 1.00 | 26 | 54 | 0.46 | 0.10 | 0.045 | 0.54 | 0.11 | 0.77 |
| 1.25 | 27 | 54 | 0.46 | 0.10 | 0.045 | 0.54 | 0.11 | 0.77 |
| 1.50 | 27 | 55 | 0.44 | 0.10 | 0.045 | 0.54 | 0.11 | 0.77 |
| 1.75 | 27 | 56 | 0.44 | 0.10 | 0.045 | 0.54 | 0.11 | 0.77 |
| 2.00 | 27 | 56 | 0.44 | 0.10 | 0.045 | 0.54 | 0.11 | 0.76 |
| 2.25 | 27 | 56 | 0.44 | 0.10 | 0.045 | 0.54 | 0.11 | 0.77 |
| 2.50 | 27 | 56 | 0.44 | 0.10 | 0.045 | 0.54 | 0.11 | 0.77 |
| 2.75 | 27 | 57 | 0.44 | 0.10 | 0.045 | 0.54 | 0.11 | 0.76 |
| 3.00 | 27 | 57 | 0.44 | 0.10 | 0.045 | 0.54 | 0.11 | 0.77 |
| 3.25 | 27 | 57 | 0.44 | 0.10 | 0.045 | 0.54 | 0.11 | 0.76 |
| 3.50 | 27 | 57 | 0.44 | 0.10 | 0.044 | 0.54 | 0.11 | 0.76 |
| 3.75 | 27 | 57 | 0.44 | 0.10 | 0.044 | 0.54 | 0.11 | 0.76 |
| 4.00 | 28 | 57 | 0.44 | 0.10 | 0.044 | 0.54 | 0.11 | 0.76 |
| 4.25 | 28 | 57 | 0.44 | 0.10 | 0.044 | 0.53 | 0.11 | 0.77 |
| 4.50 | 28 | 57 | 0.44 | 0.10 | 0.044 | 0.53 | 0.11 | 0.77 |

From the results obtained from the experiment, the temperature coefficient for the maximum current, the maximum voltage and the maximum power were determined. This was carried out by computing the ratio of change in each parameter with respect to the change in temperature [34,37]. It was calculated that the maximum current coefficient was 0.000mA/°C, the maximum voltage coefficient was 2.1875mV/°C and the maximum power coefficient was 0.2188mW/°C.

## Conclusions

A new family of CPC known as the RACPC has been proposed and one specific designed was fabricated and tested indoors. The steps to assemble a RACPC-PV cell structure have been explained in detail. This prototype underwent a series of indoor experiments and the results were compared with those of a non-concentrating panel. It has been found that the RACPC increased the maximum power ratio of the system by up to 3.33x when compared with the non-concentrating cell. Within the half-acceptance angle of the RACPC, the electrical output was always higher than the one obtained from a non-

concentrating cell, with a value of 3.01x and an optical efficiency of 84% at normal incidence. The opto-electronic gain was also compared with the simulation results and the results from the experiment showed good agreement with the ZEMAX® simulation analysis. In terms of the thermal performance of the RACPC, it was demonstrated that the maximum steady state temperature of the panel for the experimental setup used was 57°C, achieved within 2.75 hours of exposure to the sun. The corresponding maximum power during the steady state was recorded at 0.044W. The maximum voltage coefficient, the maximum current coefficient and the maximum power coefficient were determined to be 2.1875mV/°C, 0.000mA/°C and 0.2188mW/°C. It can be concluded that the RADTIRC has the potential to increase the electrical output from a non-concentrating system. Within the half-acceptance angle of the RACPC, the short circuit current and the maximum power are always higher than the ones generated from a non-concentrating system.

## Acknowledgments

This project is funded by Glasgow Caledonian University (GCU), Scotland's Energy Technology Partnership (ETP) and Majlis Amanah Rakyat (MARA), Malaysia. The authors would like to acknowledge the collaboration of AES Ltd. for its contribution to this project. Thanks are due to Mr Ian Baistow from Solar Capture Technologies Ltd, United Kingdom for providing the solar cells, Mr Antoine Y Messiou from UK Optical Plastics Limited, United Kingdom for fabricating the concentrators and Mr Mark Kragh from Off-Grid Europe, Germany for supplying the tabbing wire.

## References

[1] EPIA. Global market outlook for photovoltaics 2014-2018. 2014.

[2] REN21. Renewables 2014 Global Status Report 2014:1–214.

[3] Muhammad-Sukki F, Ramirez-Iniguez R, Abu-Bakar SH, McMeekin SG, Stewart BG. An evaluation of the installation of solar photovoltaic in residential houses in Malaysia: Past, present, and future. Energy Policy 2011;39:7975–87.

[4] Muhammad-Sukki F, Abu-Bakar SH, Munir AB, Mohd Yasin SH, Ramirez-Iniguez R, McMeekin SG, et al. Feed-in tariff for solar photovoltaic: The rise of Japan. Renewable Energy 2014;68:636–43.

449 [5] Muhammad-Sukki F, Ramirez-Iniguez R, McMeekin SG, Stewart BG, Chilukuri M V. Feed-In
450 Tariff for solar PV in Malaysia: Financial analysis and public perspective. 2011 5th
451 International Power Engineering and Optimization Conference, IEEE; 2011, p. 221–6.

452 [6] Mohd Yasin SH, Munir AB, Muhammad-Sukki F, Abu-Bakar SH, Ramirez-Iniguez R. Feed-in
453 Tariffs: Money from the Sun? International Conference on "Emerging Issues In Public Law:
454 Challenges and Perspectives" (ICPL 2011), Faculty of Law, UiTM, Malaysia: 2011, p. 1–13.

455 [7] Munir AB, Mohd Yasin SH, Muhammad-Sukki F, Abu-Bakar SH, Ramirez-Iniguez R. Feed-in
456 tariff for solar photovoltaic : Money from the sun? Malayan Law Journal 2012;2:lvii – lxxii.

457 [8] Muhammad-Sukki F, Munir AB, Ramirez-Iniguez R, Abu-Bakar SH, Mohd Yasin SH,
458 McMeekin SG, et al. Solar photovoltaic in Malaysia: The way forward. Renewable and
459 Sustainable Energy Reviews 2012;16:5232–44.

460 [9] Muhammad-Sukki F, Munir AB, Ramirez-Iniguez R, Abu-Bakar SH, Yasin SHM, McMeekin
461 SG, et al. Soft loan for domestic installation of solar photovoltaic in Malaysia: Is it the best
462 option? 2012 IEEE Business, Engineering & Industrial Applications Colloquium (BEIAC),
463 IEEE; 2012, p. 388–93.

464 [10] Muhammad-Sukki F, Munir AB, Mohd Yasin SH, Ramirez-Iniguez R, Abu-Bakar SH,
465 McMeekin SG, et al. Feed-in Tariff in Malaysia : Six Months After. Sustainable Future Energy
466 2012 & 10th Sustainable and Secure Energy (SEE) Forum 2012, Brunei: 2012, p. 452–8.

467 [11] Muhammad-Sukki F, Abu-Bakar SH, Munir AB, Mohd Yasin SH, Ramirez-Iniguez R,
468 McMeekin SG, et al. Progress of feed-in tariff in Malaysia: A year after. Energy Policy
469 2014;67:618–25.

470 [12] Muhammad-Sukki F, Ramirez-Iniguez R, Munir AB, Mohd Yasin SH, Abu-Bakar SH,
471 McMeekin SG, et al. Revised feed-in tariff for solar photovoltaic in the United Kingdom: A
472 cloudy future ahead? Energy Policy 2013;52:832–8.

473 [13] Ahmad S, Tahar RM, Muhammad-Sukki F, Munir AB, Rahim RA. Role of feed-in tariff
474 policy in promoting solar photovoltaic investments in Malaysia: A system dynamics approach.
475 Energy 2015.

476 [14] IPCC. Climate Change 2014: Mitigation of Climate Change. Contribution of Working Group
477 III to the Fifth Assessment Report of the Intergovernmental Panel on Climate Change.
478 Cambridge University Press, Cambridge, United Kingdom and New York, NY, USA.: 2014.

479 [15] IEA-PVPS. TRENDS 2014: Survey Report of Selected IEA Countries between. 2014.

480 [16] Swanson RM. The promise of concentrators. Progress in Photovoltaics: Research and
481 Applications 2000;8:93–111.

482 [17] Muhammad-Sukki F, Ramirez-iniguez R, Mcmeekin SG, Stewart BG, Clive B. Solar
483 Concentrators. International Journal of Applied Sciences 2010;1:1–15.

484 [18] Muhammad-Sukki F, Ramirez-iniguez R, McMeekin SG, Stewart BG, Clive B. Solar
485 concentrators in malaysia: Towards the development of low cost solar photovoltaic systems.
486 Jurnal Teknologi 2011;54:289–98.

[19] Fernández EF, Almonacid F, Sarmah N, Rodrigo P, Mallick TK, Pérez-Higueras P. A model based on artificial neuronal network for the prediction of the maximum power of a low concentration photovoltaic module for building integration. Solar Energy 2014;100:148–58.

[20] Sarmah N, Richards BS, Mallick TK. Design, development and indoor performance analysis of a low concentrating dielectric photovoltaic module. Solar Energy 2014;103:390–401.

[21] Sendhil Kumar N, Matty K, Rita E, Simon W, Ortrun A, Alex C, et al. Experimental validation of a heat transfer model for concentrating photovoltaic system. Applied Thermal Engineering 2012;33-34:175–82.

[22] Uematsu T, Yazawa Y, Joge T, Kokunai S. Fabrication and characterization of a flat-plate static-concentrator photovoltaic module. Solar Energy Materials and Solar Cells 2001;67:425–34.

[23] Gajbert H, Hall M, Karlsson B. Optimisation of reflector and module geometries for stationary, low-concentrating, façade-integrated photovoltaic systems. Solar Energy Materials and Solar Cells 2007;91:1788–99.

[24] García M, Marroyo L, Lorenzo E, Pérez M. Experimental energy yield in 1·5 × and 2 × PV concentrators with conventional modules. Progress in Photovoltaics: Research and Applications 2008;16:261–70.

[25] Yoshioka K, Goma S, Hayakawa S, Saitoh T. Preparation and properties of an experimental static concentrator with a new three-dimensional lens. Progress in Photovoltaics: Research and Applications 1997;5:139–45.

[26] Muhammad-Sukki F, Ramirez-Iniguez R, McMeekin S, Stewart B, Clive B. Optimised Dielectric Totally Internally Reflecting Concentrator for the Solar Photonic Optoelectronic Transformer System: Maximum Concentration Method. In: Setchi R, Jordanov I, Howlett R, Jain L, editors. Knowledge-Based and Intelligent Information and Engineering Systems SE - 67, vol. 6279, Springer Berlin Heidelberg; 2010, p. 633–41.

[27] Muhammad-Sukki F, Ramirez-iniguez R, McMeekin SG, Stewart BG, Clive B. Optimised concentrator for the Solar Photonic Optoelectronic Transformer System : First optimisation stage. International Conference on Harnessing Technology (ICHT), Muscat, Oman: 2011, p. 1–7.

[28] Muhammad-Sukki F, Ramirez-iniguez R, McMeekin SG, Stewart BG, Clive B. Optimised concentrator for the Solar Photonic Optoelectronic Transformer System : First optimisation stage. Caledonian Journal of Engineering 2011;07:19–24.

[29] Muhammad-Sukki F, Ramirez-Iniguez R, McMeekin SG, Stewart BG, Clive B. Optimisation of concentrator in the solar photonic optoelectronic transformer: optical gain analysis. IET Conference on Renewable Power Generation (RPG 2011), IET; 2011, p. P04–P04.

[30] Muhammad-Sukki F, Ramirez-Iniguez R, McMeekin SG, Stewart BG, Clive B. Optimisation of Concentrator in the Solar Photonic Optoelectronic Transformer : Comparison of Geometrical Performance and Cost of Implementation. International Conference on Renewable Energies and Power Quality (ICREPQ'11), Las Palmas de Gran Canaria, Spain: 2011, p. 1–6.

[31] Muhammad-Sukki F, Ramirez-Iniguez R, McMeekin SG, Stewart BG, Clive B. Optimisation of Concentrator in the Solar Photonic Optoelectronic Transformer : Comparison of Geometrical Performance and Cost of Implementation. Renewable Energy and Power Quality Journal and Power Quality Journal 2011;9:1–6.

[32] Ramirez-iniguez R, Muhammad-Sukki F, McMeekin SG, Stewart BG. Optical element. Patent No. 2497942, 2014.

[33] Muhammad-Sukki F, Abu-bakar SH, Ramirez-iniguez R, Mcmeekin SG, Stewart BG, Sarmah N, et al. Mirror symmetrical dielectric totally internally reflecting concentrator for building integrated photovoltaic systems. Applied Energy 2014;113:32–40.

[34] Muhammad-Sukki F, Abu-Bakar SH, Ramirez-Iniguez R, McMeekin SG, Stewart BG, Munir AB, et al. Performance analysis of a mirror symmetrical dielectric totally internally reflecting concentrator for building integrated photovoltaic systems. Applied Energy 2013;111:288–99.

[35] Ramirez-Iniguez R, Muhammad-Sukki F, Abu-Bakar SH, McMeekin SG, Stewart BG, Sarmah N, et al. Rotationally asymmetric optical concentrators for solar PV and BIPV systems. 2013 IEEE 4th International Conference on Photonics (ICP), IEEE; 2013, p. 15–7.

[36] Muhammad-Sukki F. Optimised solar concentrator for the solar photonic optoelectronic transformer system. Glasgow Caledonian University, 2013.

[37] Mammo ED, Sellami N, Mallick TK. Performance analysis of a reflective 3D crossed compound parabolic concentrating photovoltaic system for building façade integration. Progress in Photovoltaics: Research and Applications 2013;21:1095–103.

[38] Abu-Bakar SH, Muhammad-Sukki F, Ramirez-Iniguez R, Mallick TK, Munir AB, Mohd Yasin SH, et al. Rotationally asymmetrical compound parabolic concentrator for concentrating photovoltaic applications. Applied Energy 2014;136:363–72.

[39] Ning X, Winston R, O'Gallagher J. Dielectric totally internally reflecting concentrators. Applied Optics 1987;26:300–5.

[40] Messiou A. Y. UK Optical Plastics Ltd. Available from Http://www.ukopticalplastics.com/index.html - Accessed 10 Nov 2014.

[41] ARKEMA GROUP. Standard range - Altuglas® acrylic resins. Available from Http://www.altuglas.com/en/resins/resins-by-Performance/standard-Range/index.html - Accessed 10 Nov 2014.

[42] Sarmah N. Design and Performance Evaluation of a Low Concentrating Line-axis Dielectric Photovoltaic System. Heriot-Watt University, United Kingdom, 2012.

[43] Sellami N, Mallick TK, McNeil DA. Optical characterisation of 3-D static solar concentrator. Energy Conversion and Management 2012;64:579–86.

[44] Solar Capture Technologies. Cells. Available from Http://solarcapturetechnologies.com/services/manufacturing/cells - Accessed 10 Nov 2014.

[45] Honsberg C, Bowden S. 2015. PVCDROM. Available from http://www.pveducation.org/. Last accessed on 16/04/ 2015.

[46] Stine WB, Geyer M. Power from the Sun. Availabe from http://www.powerfromthesun.net/Book/chapter02/chapter02.html- Accessed 10 June 2014.

[47] Welford WT, Winston R. High Collection Nonimaging Optics. Academic Press; 1989.

[48] Tutor Vista. 2015. Available from http://www.tutorvista.com/. Last accessed on 16/04/ 2015.

[49] Kumar R, Rosen MA. A critical review of photovoltaic–thermal solar collectors for air heating. Applied Energy 2011;88:3603–14.

[50] X-Rates. 2014. Currency Calculator. Available from http://www.x-rates.com/calculator/. Last accessed on 10/11/ 2014.